Chemical Proteomic Analysis Reveals the Drugability of the Kinome of *Trypanosoma brucei*

Michael D. Urbaniak,*,[†] Toby Mathieson,[‡] Marcus Bantscheff,[‡] Dirk Eberhard,[‡] Raffaella Grimaldi,[†] Diego Miranda-Saavedra,[§] Paul Wyatt,[†] Michael A. J. Ferguson,[†] Julie Frearson,[∥] and Gerard Drewes*,[‡]

[†]Division of Biological Chemistry and Drug Discovery, College of Life Sciences, University of Dundee, Dow Street, Dundee DD1 5EH, U.K.

[‡]Cellzome AG, Meyerhofstrasse 1, D-69117 Heidelberg, Germany

[§]World Premier International Immunology Frontier Research Centre, Osaka University, 3-1 Yamadaoka, Suita 565-0871, Osaka, Japan

[∥]BioFocus, Chesterford Park, Saffron Walden, Essex CB10 1XL, U.K.

S *Supporting Information*

ABSTRACT: The protozoan parasite *Trypanosoma brucei* is the causative agent of African sleeping sickness, and there is an urgent unmet need for improved treatments. Parasite protein kinases are attractive drug targets, provided that the host and parasite kinomes are sufficiently divergent to allow specific inhibition to be achieved. Current drug discovery efforts are hampered by the fact that comprehensive assay panels for parasite targets have not yet been developed. Here, we employ a kinase-focused chemoproteomics strategy that enables the simultaneous profiling of kinase inhibitor potencies against more than 50 endogenously expressed *T. brucei* kinases in parasite cell extracts. The data reveal that *T. brucei* kinases are sensitive to typical kinase inhibitors with nanomolar potency and demonstrate the potential for the development of species-specific inhibitors.
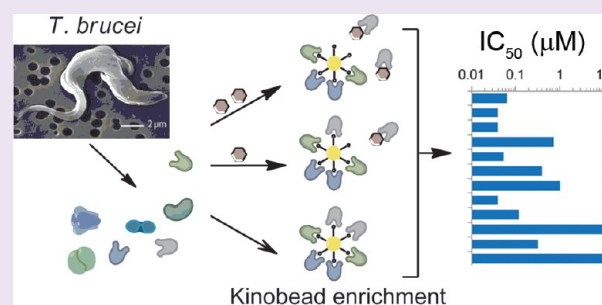
The protozoan parasite *Trypanosoma brucei* is transmitted by the bite of an infected Tsetse fly and causes African sleeping sickness, which is also known as Human African Trypanosomasis (HAT). The disease is invariably fatal if left untreated and results in upward of 10,000 deaths each year in sub-Saharan Africa.[1] *T. brucei* has a complex digenetic lifecycle between the insect vector and mammalian host, and the ability to adapt to these environments is essential to its survival and virulence. During early stages of infection the clinically relevant bloodstream form of the parasite proliferates in the blood and lymph of the human host and then in the second stage enters the cerebrospinal fluid and brain, resulting in coma and death. Current treatments are expensive, toxic, and difficult to administer, leaving an urgent unmet need for improved therapeutic agents.[2]

Protein kinases play key roles in the control of growth and cell signaling and are a major target of the pharmaceutical industry. Parasite protein kinases have been proposed as attractive targets for drug discovery as such efforts can "piggy-back" on the extensive knowledge of the development of inhibitors against human protein kinases.[3] In the case of *T. brucei*, bioinformatic analysis of the genome has identified 176–182 putative protein kinases on the basis of sequence similarity, the majority of which can be placed within well-recognized kinase groups (Supplementary Table S1).[4,5] Efforts to

determine the detailed biological role of *T. brucei* protein kinases are ongoing, although knock-down by RNA interference has provided evidence of the essential nature of a significant number of protein kinases.[6] However, the rationale to develop drugs to target the *T. brucei* kinome poses a conundrum: if mammalian and parasite protein kinases are sufficiently similar to be identified and classified on the basis of sequence similarity and are inhibited by typical inhibitors, will parasite kinase inhibitors lack host–parasite specificity? Conversely, if the kinases are sufficiently different that host–parasite specificity can be readily obtained, will they be inhibited by typical inhibitors of mammalian kinases? In other words, we need to consider the similarity of the chemical space that parasite and mammalian protein kinase inhibitors occupy, rather than the similarity in protein kinase sequence.

One way to probe the inhibitor chemical space is to profile inhibitor activity against both the mammalian and parasite kinomes. Such profiling is often achieved using *in vitro* activity assays against a panel of recombinant protein kinases,[7] but there is no such panel available for the *T. brucei* kinome; indeed only a handful of active *T. brucei* kinases have been
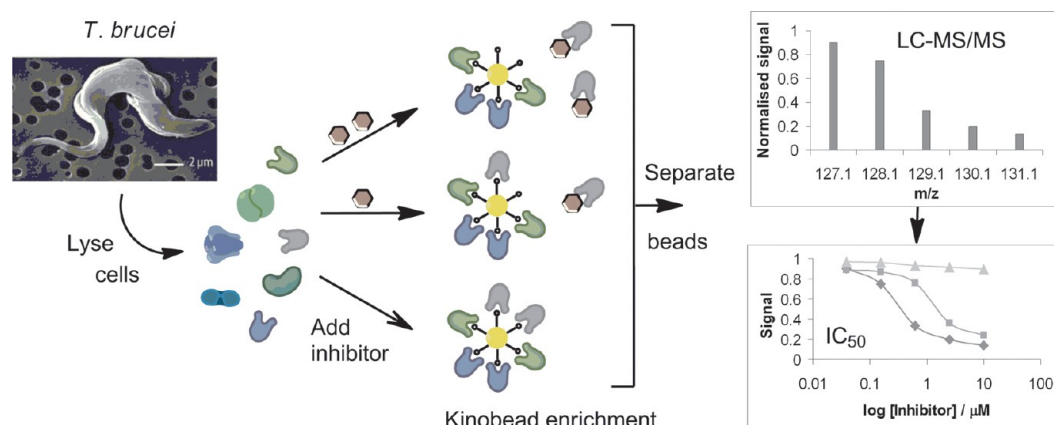
Figure 1. Chemical proteomics approach to profiling the targets of kinase inhibitors. *T. brucei* cell lysates are incubated in the presence or absence of the test inhibitor prior to the addition of mixed kinase-inhibitor beads (kinobeads) to enrich kinases and related proteins. The presence of the test kinase inhibitor prevents the binding of its target(s) to the kinobeads. Analysis of the kinobead-bound subproteome by quantitative tandem mass spectrometry using isobaric tags allows inhibition curves to be calculated for each protein observed.
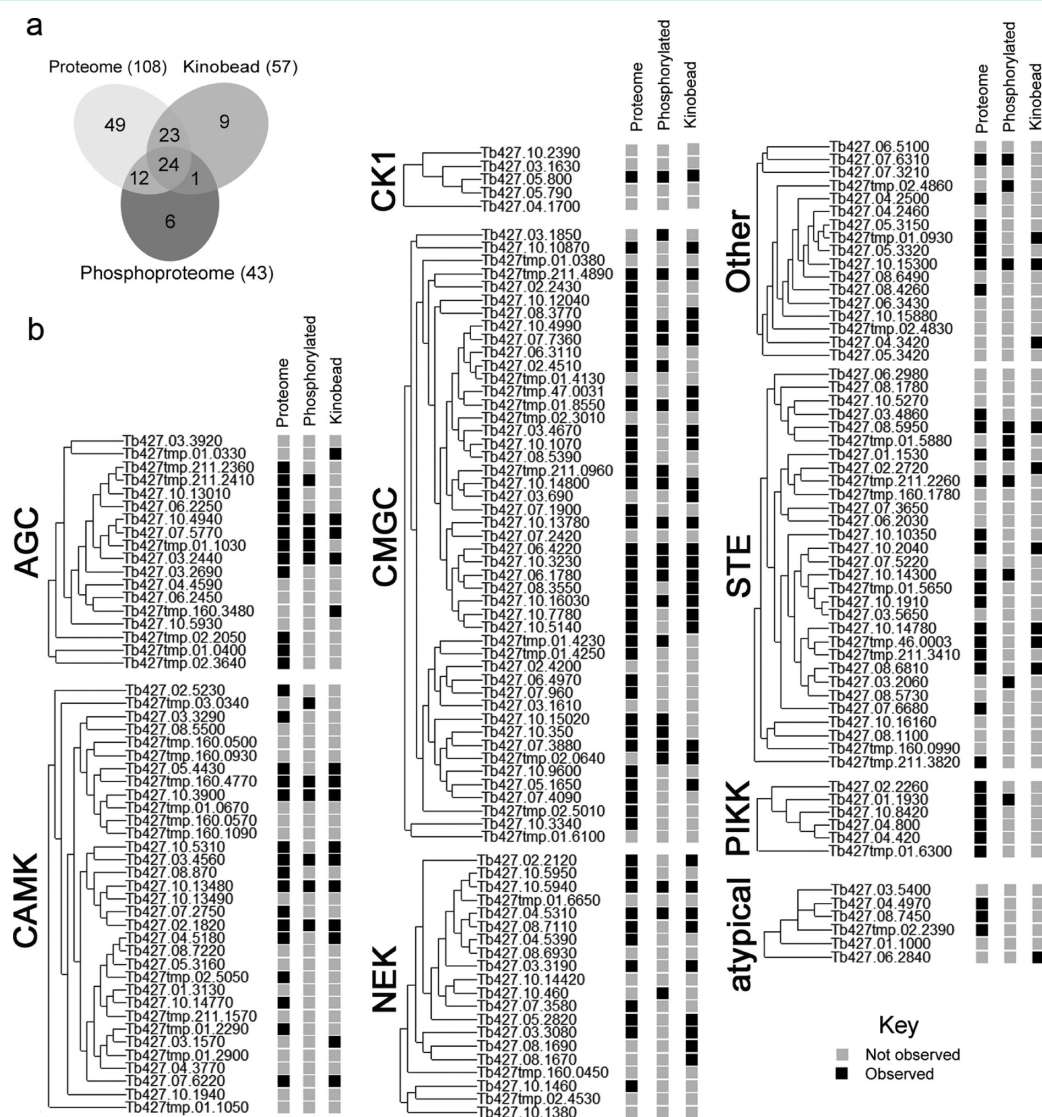

Figure 2. Profiling the kinome expressed in bloodstream form *T. brucei* using complementary mass spectrometry-based observations. (a) Venn diagram summarizing overlapping protein kinase observations. (b) Details of protein kinases observed (black square), divided by kinase group classification according to the similarity of their catalytic domains. Proteome: detection at natural abundance. Phosphorylated: enrichment of phosphorylated peptides.[5] Kinobeads: enriched by immobilized mixed kinase-inhibitors.
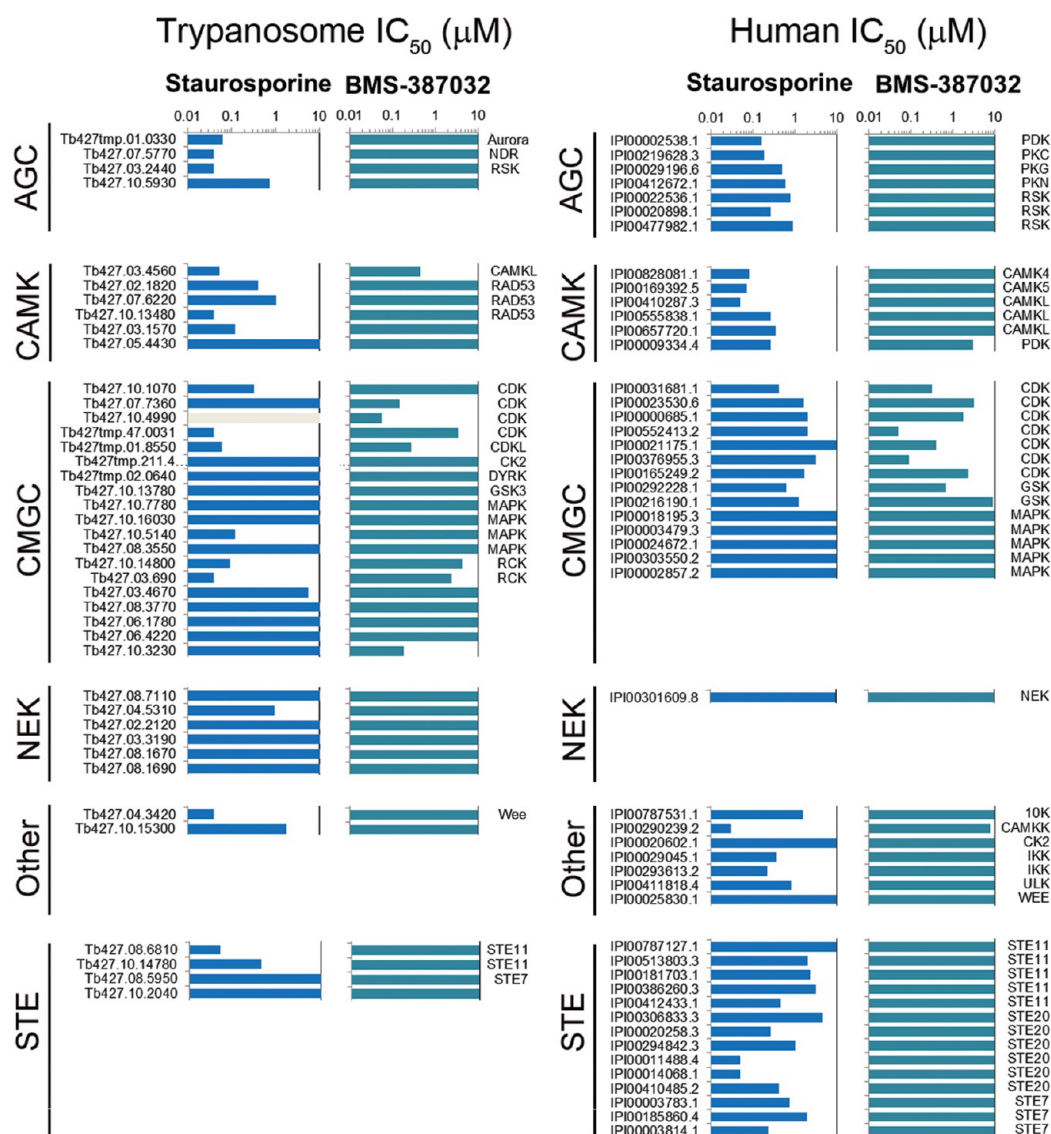
Figure 3. Chemical proteomics profiling of Staurosporine and BMS-387032 against the trypanosome and human kinome. Horizontal bars represent IC$_{50}$ value calculated from the isobaric reporter signals, gray bars indicate where binding was not quantified. Lysates were incubated with varying concentrations of compounds prior to incubation with kinobeads, and the bound fraction was quantified by tandem mass spectrometry. Data for TK, TKL, atypical, and lipid kinase are not shown for clarity; the full data for the trypanosome profile can be found in Supplementary Table S5, and the CLL cell data has been reported previously.[17]

recombinantly expressed as active enzymes.[8−10] A recent advance in kinase inhibitor profiling uses a chemical proteomic methodology that captures a substantial portion of the expressed kinome (and related proteins) contained in cell lysates on a mixed kinase-inhibitor matrix known as kinobeads.[11,12] Addition of a kinase inhibitor to the cell lysates enables it to bind to its specific target(s), occupying the binding sites and preventing binding to the kinobeads, whereas the binding of nontargeted kinases and other proteins are unaffected. Incubation of the lysate with varying concentrations of the inhibitor and subsequent analysis of the kinobead-bound subproteome by quantitative mass spectrometry allows inhibition curves to be generated for each protein observed (Figure 1). We reasoned that this methodology should be species independent, provided that the kinobeads are sufficiently promiscuous to capture a sizable portion of the parasite kinome.

Here, we present the results of our efforts to establish kinobead chemoproteomics profiling in *T. brucei* and estimate the coverage of the parasite kinome. Our strategy enabled us to access more than 50 parasite kinases for inhibitor profiling, which by far exceeds any currently available enzyme panels. We report the profile of the mammalian kinase inhibitors staurosporine and BMS-387032 and several early hit compounds identified as parasite protein kinase inhibitors by the Drug Discovery Unit at the University of Dundee.

■ **RESULTS AND DISCUSSION**

Coverage of the *T. brucei* Kinome. Kinobeads consist of immobilized analogues of a variety of ATP competitive kinase inhibitors that show relatively promiscuous binding to the mammalian kinases, but their ability to bind kinases from more divergent organisms has not been examined. To establish to what extent *T. brucei* protein kinases were able to bind to the kinobeads, we examined the subproteome enriched from cell

lysates of the clinically relevant bloodstream form of *T. brucei*. Initially, we compared four versions of kinobeads that differ in the identity of the immobilized inhibitors (see Methods). In these experiments, we observed the enrichment of a total of a 57 protein kinases (Supplementary Table S2). The enrichment of a significant number of trypanosome protein kinases by these promiscuous mammalian kinase inhibitors suggests that the ATP binding pocket architecture is broadly conserved between the two species.

Estimating the portion of the trypanosome kinome captured is not straightforward, as the bloodstream form represents just one of the multiple lifecycle stages of *T. brucei* and may not express every kinase encoded by the genome. Before we could determine the proportion of the bloodstream form kinome that was captured by kinobeads, we needed to estimate how many protein kinases were present in the cell lysates. To achieve this, we took advantage of the differing bias of two orthogonal proteomic techniques. By analyzing the total proteome contained in the non-enriched cell lysate we identified the most abundant 3248 proteins, which included 90 protein kinases (Supplementary Table S3). This data shows good overlap with a recent comparative SILAC proteomic study of the bloodstream and procyclic form *T. brucei*, which identified 65 protein kinases,[13] including 18 not seen in this study. A separate phosphoproteomic study by Nett *et al.*,[5] which used strong cation exchange and TiO_2 chromatography to enrich for phosphopeptides, identified 43 phosphorylated protein kinases in bloodstream form *T. brucei*. Comparison of the protein kinases identified by these three orthogonal proteomics techniques revealed overlapping and complementary coverage of the bloodstream form kinome (Figure 2 and Supplementary Table S4), providing experimental observation of a total of 124 protein kinases out of the predicted 182 (68%). The kinases that bind to kinobeads are not significantly biased toward abundant (Supplementary Figure S1) or phosphorylated protein kinases or any particular kinase group. Mapping the kinases that bind to kinobeads onto the phylogeny of the *T. brucei* kinome shows that kinobead enrichment appears to be independent of the degree of sequence homology (Figure 2). While it is likely that the coverage of this observable bloodstream form kinome is not complete, it is in reasonable agreement with transcriptome studies that suggest 25% of the genome is differentially expressed between bloodstream and procyclic form *T. brucei* cells.[14] The kinobead-enriched subproteome contains 46% of the observed bloodstream form kinome (31% of the predicted genome), comparable to the coverage obtained from analysis of human cell lysates (52% of the predicted genome).

Profiling of Known Kinase Inhibitors. Kinobead-based profiling enables access to a sizable fraction of the expressed trypanosome kinome, which can be used to determine the potency and selectivity of kinase inhibitors in cell extracts by means of a multiplexed competition binding assay. The kinobeads version producing the best coverage of the *T. brucei* kinome was used to determine the kinase inhibition profile of two well-studied kinase inhibitors: Staurosporine and BMS-387032. The binding of these inhibitors to their cellular targets was quantified by mass spectrometry using isobaric tags for relative and absolute quantification (iTRAQ)[15,16] for 51 protein kinases and 67 other kinobead-binding proteins (Figure 3 and Supplementary Table S5). Staurosporine, a natural product, is a prototypical ATP-competitive pan-kinase inhibitor that binds to many protein kinases with high affinity and little selectivity.[11] In

a previous study we reported kinobead profiling of staurosporine in primary chronic lymphocytic leukemia cells[17] and demonstrated that more than a third of the observed human kinome (41/112) displayed submicromolar IC_{50} values (Figure 3). This pan-kinase activity was retained against the *T. brucei* kinome, with more than a third of the observed trypanosome kinome (18/44) displaying IC_{50} values <1 μM, including 10 with IC_{50} values below 100 nM (Figure 3).

The second kinase inhibitor to be profiled, BMS-387032, an established pan-cyclin-dependent kinase (CDK) inhibitor, was selected because *T. brucei* have a relatively expanded CMGC group including many putative CDK or CDK-like (CDKL) family members.[4,5] Kinobead profiling of BMS-387032 against primary chronic lymphocytic leukemia cells showed that all of the seven observed CDKs were inhibited, with CDK2, CDK9, CRK7, and PCSTAIRE2 displaying submicromolar IC_{50} values (Figure 3).[17] BMS-387032 retained the ability to inhibit the majority of the observed trypanosome CDKs, including targeting the CDK2-related kinases CRK2 and CRK3 with submicromolar potency (IC_{50} of 148 and 57 nM, respectively), although no inhibition of CRK1 was observed (Figure 3). In addition, the compound selectivity was slightly broader than just the CDKs, with two additional kinases (CMGC and CAMK) also inhibited with IC_{50} values below 500 nM, which may reflect the divergence of the trypanosome kinome. These data provide the first molecular evidence that the trypanosome kinome is sensitive to typical mammalian kinases inhibitors with nanomolar potencies and suggest that other standard kinase inhibitor scaffolds may retain substantial activity.

Profiling Trypanosome Kinase Inhibitors. The Drug Discovery Unit at the University of Dundee has conducted a number of screening campaigns to help identify preclinical candidates for the treatment of African sleeping sickness, including target-based screens against the *T. brucei* protein kinases Glycogen Synthase Kinase 3 (GSK3, Tb427.10.13780) and the Nuclear DBF-2-related (NDR) kinases PK50 (Tb427.10.4940) and PK53 (Tb427.07.5770).[8] Details of the compound screening and optimization will be reported elsewhere. To further probe the chemical space that mammalian and trypanosome kinase inhibitors occupy and demonstrate the utility of chemical proteomics in antiparasitic drug discovery, we profiled hits selected from these screens (Supplementary Tables S6 and S7). The compounds selected all show nanomolar potency against their respective molecular target *in vitro* and variable efficacy against cultured trypanosome and human hepatocyte (MRC5) cells (Table 1).

Table 1. Trypanosome Kinase Inhibitors

	GSK3	PK50	PK53
compound ID	DDD85893	DDD34425	DDD88213
T. brucei enzyme IC_{50} (μM)[a]	<0.002	0.013 ± 0.006	0.73 ± 0.14
T. brucei kinobead IC_{50} (μM)[b]	<0.039	not observed	5.7
T. brucei EC_{50} (μM)[c]	1.3 ± 1.2	0.86 ± 0.52	45 ± 4
H. sapiens MRC5 EC_{50} (μM)[c]	28 ± 9.7	>50	>50
H. sapiens kinobead IC_{50} (μM)[b]	<0.06	not observed	not observed

[a]Enzyme IC_{50} values were determined using a plate-based radiometric assay. [b]Kinobead IC_{50} is described in Methods. [c]Cell EC_{50} values were determined using an Alamar blue assay.[34]
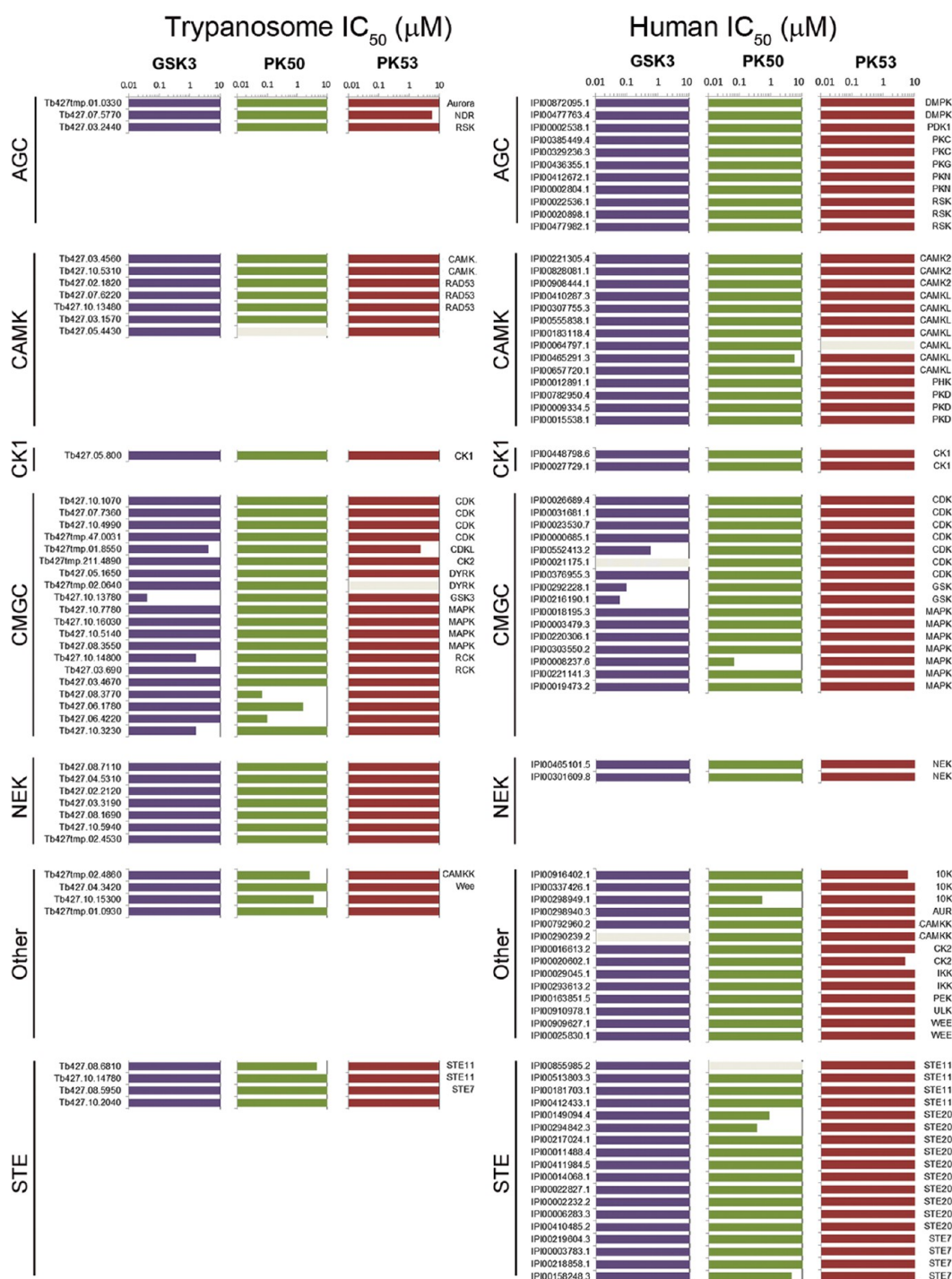
Figure 4. Chemical proteomics profiling of trypanosome kinase inhibitors against the kinome of bloodstream form *T. brucei*. Horizontal bars represent IC$_{50}$ value calculated from the isobaric reporter signals; gray bars indicate where binding was not quantified. Lysates were incubated with varying concentrations of compounds prior to incubation with kinobeads, and the bound fraction was quantified by tandem mass spectrometry. Data for TK, TKL, atypical, and lipid kinase are not shown for clarity; the full data can be found in Supplementary Tables S6 and S7.

The compound DDD85893 was identified as a potent inhibitor of *T. brucei* GSK3 (TbGSK3) *in vitro*, with good efficacy against cultured *T. brucei* and good selectivity against cultured human cells. The kinobead profiling of DDD85893 against *T. brucei* cell lysates confirmed that TbGSK3 was inhibited with nanomolar potency, with three other CMGC kinases inhibited at micromolar level (Figure 4). The compound also showed a very clean profile against human MRC5 cell lysates, with only human GSK3α, GSK3β, and

CDK9 inhibited with nanomolar potency. These data show that the compound DDD85893 has excellent selectivity for GSK3 and limited other CMGC members but does not display any species specificity.

The second compound to be profiled (DDD34425) was identified as a potent inhibitor of *T. brucei* PK50 *in vitro*, with good efficacy against cultured *T. brucei* and good selectivity against cultured human cells. Unfortunately, the expected target PK50 was not among the kinases that bound to the kinobeads,

suggesting that the ATP binding site contains features that are not recognized by the set of standard ligands immobilized on the beads. Indeed, none of the four human NDR kinases (NDR1, NDR2, LATS1, LATS2) were among the kinases in MRC5 lysates that bound to the kinobeads. However, the kinobead profile of DDD34425 against *T. brucei* cell lysates revealed that MAPK10 and MAPK5 were inhibited with nanomolar potency, with three other kinases inhibited at micromolar level (Figure 4). As *T. brucei* bloodstream form MAPK5 null mutants grow normally *in vitro*[18] and little is known about MAPK10,[19] it is unclear what effect, if any, their inhibition may contribute to the observed trypanocidal effect of DDD34425. The kinobead profile against MRC5 cell lysates showed a broader specificity, with the MAPK NKL and TKLs RIPK2 and ALK2 inhibited with nanomolar potency. Six additional kinases from four different groups were inhibited at the micromolar level. These data revealed that the compound DDD34425 lacks specificity against the observable trypanosome kinome and significant poly pharmacology against the observable human kinome, including a number of tyrosine-specific kinases that are absent from *T. brucei*.

The compound DDD88213 was identified as a submicromolar inhibitor of *T. brucei* PK53 *in vitro* but lacked efficacy against both cultured *T. brucei* and human cells. The kinobeads profile of DDD88213 against *T. brucei* cell lysates revealed that PK53 was inhibited with an IC$_{50}$ of 5.7 μM, with CK2α2 also inhibited with similar potency (Figure 4). The 10-fold drop in potency between the enzyme IC$_{50}$ and the kinobeads binding assay is not significantly different from that seen with other inhibitors and may reflect differences between purified proteins and cell extracts. Moreover, the potency determined with kinobeads is in line with the weak activity of the compound in the Alamar blue assay. The kinobead profile against MRC5 cell lysates showed that none of the observable human kinome was significantly inhibited by DDD88213. These data show that while this compound does appear to be specifically targeting the desired trypanosome kinase and appears to have little effect on the human kinome, it lacks sufficient potency to achieve the desired trypanocidal effect and would require further optimization.

The final compound to be profiled was recently identified as a potent inhibitor of the *Leishmania major* cyclin dependent kinase 2-related kinase 3 (LmCRK3) (compound **33**, Cleghorn et al.[20]) but lacked efficacy against cultured *L. major* or the related parasite *T. brucei*.[20] As active recombinant *T. brucei* CRK3 (TbCRK3) is not available for *in vitro* screening, we attempted to use kinobead profiling to investigate whether the lack of cellular potency against *T. brucei* was due to lack of potency against TbCRK3. The kinobead profile of the compound revealed that none of the observed *T. brucei* kinases were significantly inhibited, including TbCRK3, and neither were any mammalian kinase (Supplementary Tables S6 and S7). The complete lack of inhibition suggests that the native state of parasite CRK3s is distinct from the recombinant form used for *in vitro* screening. While these differences may be due to the absence of the associated cyclin, a recent screen against LmCRK3-cyclin 6 also resulted in compounds that lacked efficacy against cultured *L. major*.[21]

Summary and Conclusions. We set out to examine the similarity of the chemical space that parasite and mammalian protein kinase inhibitors occupy using a recently developed chemical proteomics approach to profile kinase inhibitors. The data presented here represent the first molecular evidence that typical ATP-competitive inhibitors can retain low nanomolar potency against *T. brucei* protein kinases. The inhibition profile of the compounds does not seem to map directly between the two species, suggesting that it may be possible to exploit these differences to obtain host/parasite specificity. It is also possible that the differences observed are an artifact due to the limited coverage of the kinome achieved by kinobead enrichment. However, the lack of bias in the enriched kinome suggested that this is unlikely.

Our data suggest that phenotypic screening of known kinase inhibitors against *T. brucei* is likely to identify potent compounds but also show that it is inappropriate to infer the molecular target on the basis of the inhibition profile established in mammalian systems. The chemoproteomics approach presented to profile potential kinase inhibitors simultaneously covers as much as half the observed bloodstream form kinome, representing a 10-fold increase in the selection of active parasite kinases currently available for drug discovery. Development of kinobeads tailored to the trypanosome kinome, for instance, by immobilizing novel inhibitors identified through phenotypic screening, is an attractive approach to extend the coverage of the parasite kinome. Importantly, the approach presented here is species-independent and can be applied to any clinically relevant pathogen for which a genome sequence is available.

■ METHODS

Reagents and Drugs. All reagents were purchased from Sigma unless otherwise noted. Staurosporine was purchased from IRIS Biotech, and BMS-387032 was custom synthesized by Park Place Research.

Preparation of Bloodstream Form *T. brucei* Cell Lysates. Bloodstream form *T. brucei brucei* variant 117 (MITat1.4) was purified from infected rodent blood over DE52 cellulose as described previously.[22] The cells were centrifuged at $800 \times g$ for 10 min at 4 °C and resuspended at 1×10^9 cells/mL in ice-cold buffer 1 containing protease and phosphatase inhibitors (0.1 mM TLCK, 1 μg/mL Leupeptin, 1 μg/mL aprotinin, 1 mM PMSF, 1 mM benzamidine, Phosphatase Inhibitor Cocktail II (Roche)), and hypotonic lysis was allowed to proceed for 10 min on ice. An equal volume of ice-cold buffer 2 (100 mM Tris pH 7.5, 10% glycerol, 300 mM NaCl, 50 mM NaF, 3 mM MgCl$_2$, 0.2 mM Na$_3$VO$_4$, 1.6% Igepal-CA630, 2 mM DTT, 0.1 mM TLCK) was added, and the lysate was centrifuged at $145,000 \times g$ for 1 h at 4 °C. The BCA assay (Pierce) was used to determine the total protein content in the supernatant, and the concentration was adjusted to 5 mg/mL. Aliquots were frozen in liquid nitrogen and stored at −80 °C prior to use.

Preparation of *H. sapiens* MRC5 Cell Lysates. MRC5 cells were grown at 37 °C, 5% CO$_2$ in MEM supplemented with 10% FCS. Cell lysates were prepared washing the cells briefly in PBS, incubating with an equal volume of buffers 1 and 2 for 15 min, and then processing the crude lysate as described above.

Proteomic Analysis. The total proteome was determined in duplicate by fractionating 25 μg of the bloodstream form *T. brucei* cell lysate by SDS-PAGE and pixilation into 24 bands, followed by in-gel reductive alkylation and tryptic digest. Samples were analyzed by liquid chromatography − tandem mass spectrometry on a Eksigent 1D+ HPLC system coupled to a LTQ-Orbitrap mass spectrometer (Thermo scientific). MS spectra were searched using Mascot (Matrix Science) against a nonredundant, in-house compiled database of *Trypanosoma brucei* 927 and 427 strains obtained from TriTrypDB 3.0[23] with additional protein sequences from SwissProt and RefSeq databases, as well as known contaminant sequences such as keratins and trypsin. To assess the false discovery rate (FDR) "decoy" proteins (reverse of the protein sequence) were added to the database. Protein identifications were accepted as follows: (i) For single spectrum to sequence assignments, we required the assignment to be the best

match and a minimum Mascot score of 37 and a 10× difference of the assignment over the next best assignment. On the basis of these criteria, the decoy search results indicated <1% false discovery rate (FDR). (ii) For multiple spectrum to sequence assignments and using the same parameters, the decoy search results indicate <0.1% FDR. To make our data accessible to the scientific community, we have uploaded the results of this study to TriTrypDB (http://www.tritrypdb.org).[23]

Kinobead Profiling. Procedures are essentially as described previously.[11,17,24] Kinobeads were prepared by immobilization of ATP-mimetics on sepharose beads, with the four versions differing in the identity of the immobilized kinase ligands, as described in Supplementary Table S8.

For kinobead profiling, compounds were dissolved in DMSO, added at various concentrations (0, 0.039, 0.156, 0.625, 2.5, and 10 μM) to 1-mL cell lysate samples, and incubated for 45 min at 4 °C. Subsequently, kinobeads were added to each sample and incubated for a further 60 min at 4 °C. The kinobeads were collected by centrifugation and washed with lysis buffer containing 0.2% Igepal-CA630, and bead-bound proteins were eluted with NuPAGE LDS buffer (Invitrogen) containing 50 mM DTT for 30 min at 50 °C followed by alkylation with 20 mg/mL iodoacetamide for 30 min. Samples were purified on 4−12% NuPAGE gels, stained with colloidal Coomassie blue, digested with trypsin, and subsequently labeled with TMT isobaric tagging reagents (ThermoFisher Scientific).[15] Tryptic peptides were separated over 4 h using nanoflow reversed-phase chromatography online coupled to an Orbitrap mass spectrometer. Peptide fragmentation was performed using PQD, and peptides were identified with Mascot and quantified as described.[25]

Identification of the *T. brucei* 427 Strain Kinome. The annotated proteins from *T. brucei brucei* 427 strain was obtained from TriTrypDB 3.0[23] and scanned through a highly sensitive and specific multilevel HMM library of the protein kinase superfamily,[26] followed by expert curation. Assignment of putative protein kinases to the main ePK and aPK groups was done by using the *E*-value cutoffs specific for each group as described previously.[26,27] This procedure identified and assigned 187 protein kinases (Supplementary Table S1).

Phylogenetic Analysis. The phylogeny of the kinase groups identified in *T. brucei* 427 strain was determined using the Phylogeny.fr platform[28] and comprised the following steps: Sequences were aligned with T-Coffee (v6.85) using pairwise alignment methods,[29] and ambiguous regions (*i.e.*, containing gaps and/or poorly aligned) were removed with Gblocks (v0.91b)[30] with low stringency (Min. seq. for flank pos.: 55%, Max. contig. nonconserved pos.: 8, Min. block length: 5, Gaps in final blocks: half). The phylogenetic tree was reconstructed using the maximum likelihood method implemented in the PhyML program (v3.0 aLRT)[31] with reliability for internal branch assessed using the aLRT test (minimum of SH-like and Chi2-based parametric).[32] Graphical representation and editing of the phylogenetic tree was performed with TreeDyn (v198.3).[33]

ASSOCIATED CONTENT

ⓢ Supporting Information

This material is free *via* the Internet at http://pubs.acs.org.

AUTHOR INFORMATION

Corresponding Author

*E-mail: m.d.urbaniak@dundee.ac.uk; gerard.c.drewes@gsk.com.

Notes

The authors declare the following competing financial interest(s): The authors T.M., D.E., M.B., and G.D. are employees of Cellzome AG, which contributed to the funding of this work by payment-in-kind.

REFERENCES

(1) Simarro, P., Diarra, A., Ruiz Postigo, J., Franco, J., and Jannin, J. (2011) The Human African Trypanosomiasis control and Surveillance Programme of the WHO 2000−2009: The Way Forward. *PLoS Negl. Trop. Dis. 5*, e1007.

(2) Frearson, J. A., Wyatt, P. G., Gilbert, I. H., and Fairlamb, A. H. (2007) Target assessment for antiparasitic drug discovery. *Trends Parasitol. 23*, 589−595.

(3) Naula, C., Parsons, M., and Mottram, J. C. (2005) Protein kinases as drug targets in *Trypanosomes* and *Leishmania. Biochem. Biophys. Acta 1754*, 151−159.

(4) Parsons, M., Worthey, E. A., Ward, P. N., and Mottram, J. C. (2005) Comparative analysis of the kinomes of three pathogenic trypanosomatids: *Leishmania major, Trypanosoma brucei* and *Trypanosoma cruzi. BMC Genomics 6*, 127−146.

(5) Nett, I. R. E., Martin, D. M. A., Miranda-Saavedra, D., Lamont, D., Barber, J. D., Mehlert, A., and Ferguson, M. A. J. (2009) The phopshoproteome of bloodstream form *Trypanosoma brucei*, causative agent of African sleeping sickness. *Mol. Cell. Proteomics 8*, 1527−1538.

(6) Alsford, S., Turner, D. J., Obado, S. O., Sanchez-Flores, A., Glover, L., Berriman, M., Hertz-Fowler, C., and Horn, D. (2011) High-Throughput phenotyping using parallel sequencing of RNA interference targets in the African Trypanosome. *Genome Res. 21*, 915−924.

(7) Davies, S. P., Reddy, H., Caivano, M., and Cohen, P. (2000) Specificity and mechanism of action of some commonly used protein kinase inhibitors. *Biochem. J. 351*, 95−105.

(8) Ma, J., Benz, C., Grimaldi, R., Stockdale, C., Wyatt, P., Frearson, J., and Hammarton, T. C. (2010) Nuclear DBF-2-related kinases are essential regulators of cytokinesis in bloodstream stage *Trypanosoma brucei. J. Biol. Chem. 285*, 15356−15368.

(9) Urbaniak, M. D. (2009) Casein kinase 1 isoform 2 is essential for bloodstream form *Trypanosoma brucei. Mol. Biochem. Parasitol. 166*, 183−185.

(10) Ojo, K. K., Gillespie, J. R., Reichers, A. J., Napuli, A. J., Verlinde, C. L., Buckner, F. S., Gelb, M. H., Domostoj, M. M., Wells, S. J., Scheer, A., Wells, T. N., and Van Voorhis, W. C. (2008) Glycogen synthase kinase 3 is a potential drug target for African trypanosomiasis therapy. *Antimicrob. Agents Chemother. 52*, 3710−3717.

(11) Bantscheff, M., Eberhard, D., Abraham, Y., Bastuck, S., Boesche, M., Hobson, S., Mathieson, T., Perrin, J., Raida, M., Rau, C., Reader, V., Sweetman, G., Bauer, A., Bouwmeester, T., Hopf, C., Kruse, U., Neubauer, G., Ramsden, N., Rick, J., Kuster, B., and Drewes, G. (2007) Quantitative chemical proteomics reveals mechanisms of action of clinical ABL kinase inhibitors. *Nat. Biotechnol. 25*, 1035−1044.

(12) Bantscheff, M., and Drewes, G. (2012) Chemoproteomic approaches to drug target identification and drug profiling. *Bioorg. Med. Chem. 20*, 1973−1978.

(13) Urbaniak, M. D., Guther, M. L. S., and Ferguson, M. A. J. (2012) Comparative SILAC proteomic analysis of *Trypanosoma brucei* bloodstream and procyclic lifecycle stages. *PLoS One 7*, e36619.

(14) Jensen, B. C., Sivam, D., Kifer, C. T., Myler, P. J., and Parsons, M. (2009) Widespread variation in transcript abundance within and across developmental stages of *Trypanosoma brucei. BMC Genomics 10*, 482.

(15) Thomson, A., Schafer, J., Kuhn, K., Kienle, S., Schwarz, J., Schmidt, G., Naeumann, T., Johnstone, R., Mohammed, A. K., and Hamon, C. (2003) Tandem mass tags: a novel quantification stratergy for comparative analysis of complex protein mixtures by MS/MS. *Anal. Chem. 75*, 1895−1904.

1864

dx.doi.org/10.1021/cb300326z | *ACS Chem. Biol.* 2012, 7, 1858−1865

(16) Ross, P., Huang, Y., Marchese, J., Williamson, B., Parker, K., Hattan, S., Khainovski, N., Pillai, S., Dey, S., Daniels, S., Purkayastha, S., Junhasz, P., Martin, S., Bartlet-Jones, M., He, F., Jacobson, A., and Pappin, D. (2004) Multiplexed protein quantitation in *Saccharomyces cerevisiae* using amine-reactive isobaric tagging reagents. *Mol. Cell. Proteomics 3*, 1154−1169.

(17) Kruse, U., Pallasch, C. P., Bantscheff, M., Eberhard, D., Frenzel, L., Ghidelli, S., Maier, S. K., Werner, T., and Wendtner, C. M. (2011) Chemoproteomics-based kinome profling and target deconvolution of clinical multi-kinase inhibitors in primary lymphocytic leukemia cells. *Leukemia 25*, 89−100.

(18) Pfister, D. D., Burklard, G., Morand, S., Renggli, C. K., Roditi, I., and Vassella, E. (2006) A mitogen-activated protein kinase controls differentiation of bloodstream forms of *Trypanosoma brucei. Eukaryotic Cell 5*, 1126−1135.

(19) Rotureau, B., Morales, M. A., Bastin, P., and Spath, G. F. (2009) The flagellum-mitogen-activated protein kinase connection in Trypanosomatids: a key sensory role in parasite signalling and development? *Cell. Microbiol. 11*, 710−718.

(20) Cleghorn, L. A., Woodland, A., Collie, I. T., Torrie, L. S., Norcross, N., Luksch, T., Mpamhanga, C., Walker, R. G., Mottram, J. C., Brenk, R., Frearson, J. A., Gilbert, I. H., and Wyatt, P. G. (2011) Identification of inhibitors of the Leishmania cdc2-related protein kinase CRK3. *ChemMedChem 6*, 2214−2224.

(21) Walker, R. G., Thomson, G., Malone, K., Nowicki, M. W., Brown, E., Blake, D. G., Turner, N. J., Walkinshaw, M. D., Grant, K. M., and Mottram, J. C. (2011) High throughput screening yield small molecule inhibitors of Leishmania CRK3:CYC6 cyclin-dependant kinase. *PLoS Negl. Trop. Dis. 5*, e1033.

(22) Cross, G. A. M. (1984) Release and purification of *Trypanosoma brucei* variant surface glycoprotein. *J. Cell. Biochem. 24*, 79−90.

(23) Aslett, M., Aurrecoechea, C., Berriman, M., Brestelli, J., Brunk, B. P., Carrington, M., Depledge, D. P., Fischer, S., Gajria, B., Gao, X., Gardner, M. J., Gingle, A., Grant, G., Harb, O. S., Heiges, M., Hertz-Fowler, C., Houston, R., Innamorato, F., Iodice, J., Kissinger, J. C., Kraemer, E., Li, W., Logan, F. J., Miller, J. A., Mitra, S., Myler, P. J., Nayak, V., Pennington, C., Phan, I., Pinney, D. F., Ramasamy, G., Rogers, M. B., Roos, D. S., Ross, C., Sivam, D., Smith, D. F., Srinivasamoorthy, G., Stoeckert, C. J., Jr., Subramanian, S., Thibodeau, R., Tivey, A., Treatman, C., Velarde, G., and Wang, H. (2010) TriTrypDB: a functional genomic resource for the Trypanosomatidae. *Nucleic Acid Res. 38*, D457−D462.

(24) Bergamini, G., Bell, K., Shimamura, S., Werner, T., Cansfield, A., Mueller, K., Perrin, J., Rau, C., Ellard, K., Hopf, C., Doce, C., Leggate, D., Mangano, R., Mathieson, T., O'Mahony, A., Plavec, I., Rharbaoui, F., Reinhard, F., Savitski, M. M., Ramsden, N., Hirsch, E., Drewes, G., Rausch, O., Bantscheff, M., and Neubauer, G. (2012) A selective inhibitor reveals PI3Kγ dependence of T$_H$17 cell differentiation. *Nat. Chem. Biol. 8*, 576−582.

(25) Bantscheff, M., Boesche, M., Eberhard, D., Matthieson, T., Sweetman, G., and B., K. (2008) Robust and sensitive iTRAQ quantification on an LTQ Orbitrap mass spectrometer. *Mol. Cell. Proteomics 7*, 1702−1713.

(26) Miranda-Saavedra, D., and Barton, G. J. (2007) Classification and functional annotation of eukaryotic protein kinases. *Proteins 68*, 893−914.

(27) Martin, D. M., Miranda-Saavedra, D., and Barton, G. J. (2009) Kinomer v.1.0: a database of systematically classified eukaryotic protein kinases. *Nucleic Acid Res. 37*, D244−250.

(28) Dereeper, A., Guignon, V., Blanc, G., Audic, S., Buffet, S., Chevenet, F., Dufayard, J. F., Guindon, S., Lefort, V., Lescot, M., Claverie, J. M., and Gascuel, O. (2008) Phylogeny.fr: robust phylogentic analysis for the non-specialist. *Nucleic Acid Res. 36*, 36.

(29) Notredame, C., Higgins, D., and Heringa, J. (2000) T-Coffee: A novel method for multiple sequence alignment. *J. Mol. Biol. 302*, 205−217.

(30) Castresana, J. (2000) Selection of conserved blocks from multiple alignments for their use in phylogenetic analysis. *Mol. Biol. Evol. 17*, 540−552.

(31) Guindon, S., and Gascuel, O. (2003) A simple, fast, and accurate algorithm to estimate large phylogenies by maximum likelihood. *Syst. Biol. 52*, 696−704.

(32) Anisimova, M., and Gascuel, O. (2006) Approximate likelihood ration test for branches: a fast, accurate and powerful alternative. *Syst. Biol. 55*, 539−552.

(33) Chevenet, F., Brun, C., Banuls, A. L., Jacq, B., and Chisten, R. (2006) TreeDyn: towards dynamic graphic and annotation analyses of trees. *BMC Bioinfomatics 7*, 439.

(34) Durrant, J. D., Urbaniak, M. D., Ferguson, M. A. J., and McCammon, J. A. (2010) Computer-aided identification of *Trypanosoma brucei* uridine diphosphatase galactose 4′-epimerase inhibitors: towards the development of novel therapies for African sleeping sickness. *J. Med. Chem. 53*, 5025−5032.